Interaction between East Asian summer monsoon and westlies as shown by tree-ring records

Xiao Shengchun[1*], Peng Xiaomei[1], Tian Quanyan[1], Ding Aijun[2], Xie Jiali[1], Su Jingrong[1,3]

[1] Key Laboratory of Ecological Safety and Sustainable Development in Arid Lands, Northwest Institute of Eco-Environment and Resources, Chinese Academy of Sciences, Lanzhou, Gansu, China 730000.

[2] College of Resources and Environment, Gansu Agricultural University, Lanzhou, Gansu, China 730070.

[3] University of Chinese Academy of Sciences, Beijing, China 100049.

* Corresponding author (xiaosc@lzb.ac.cn).

Address: 320 West Donggang Road, Lanzhou City, Gansu Province, China.

Zip Code: 730000.

Abstract:

Atmospheric circulation changes, their driving mechanisms and interactions are important topics in global change research. Local changes in the East Asian summer monsoon (EASM) and the mid-latitude westlies will inevitably affect the climate and ecology of the arid zone of Northwest China. Hence, it is important to study these regional changes. While previous studies in this area are all single-point climate reconstruction studies, there is a lack of research on the interaction areas and driving mechanisms of the two major circulations. Dendroclimatology can provide high-resolution, long-term, and reliable multi-point proxies for the study of inter-annual and inter-decadal climate change. We chose to observe these changes in the Alxa Plateau using dendrochronological methods. We assembled ring-width records of Qinghai spruce (*Picea crassifolia*) in the mountain regions surrounding the Alxa Plateau: the Helan Mountains, Changling Mountain, and Dongdashan Mountain. The results show that radial growth was indeed affected by changes in the monsoon and westerlies. The heterogeneity of precipitation and climatic wet-dry changes in different regions is primarily influenced by the interactions between atmospheric circulation systems, each with its own dominant controlling factors. In the case of the Helan Mountains, both of these major atmospheric circulation systems play a significant role in shaping climate changes. Changling Mountain in the southern part of the Alxa Plateau is mainly influenced by the EASM. Dongdashan Mountain is mainly influenced by the westerlies. Understanding these local conditions will help us predict climate changes in Northwest China.

Key words: Alxa Plateau, dendroclimatology, westerlies, EASM, interaction between winds and monsoon.

Short summary:

Tree-rings of Qinghai spruce are a good record of regional climate change. The influence of the East Asian Summer Monsoon (EASM) and westerlies on regional dry-wet climate changes is characterized by spatio-temporal heterogeneity. The most

dramatic interplay between EASM and westerlies is observed in the Helan Mountains. Regional climate changes around Changling Mountains are most influenced by EASM, and around Dongdashan Mountain are most influenced by westerlies.

1. Introduction

The alpine zone of Qinghai-Tibet, the arid zone of the northwestern interior, and the humid zone of the east constitute the three main areas of China's natural geomorphology (Chen et al., 2019a). The Northwest China inland dry zone is located in the hinterland of the Eurasian continent and is among the driest regions in the world. It displays typical climatic characteristics of a continental climate. This region is mainly influenced by the westlies and the East Asian summer monsoon (EASM). The interaction of these two factors results in high precipitation variability and hence frequent droughts. This was true even before the onset of global climate change in the area, and it is even more pronounced in recent years. This inland arid zone is ecologically fragile (Chen et al., 2019a; Chen et al., 2019b; Zhang et al., 2023).

The semi-arid and arid regions of northern China are characterized by large areas of sand and desert. They are the second largest source of dust in the world after the Sahara. Their contribution to global climate change is large. So far inland, the influence of the EASM is often weak (Zhang et al., 2021; Liu et al., 2022). It is opposed by the westerlies that flow from the North Atlantic climate zone toward the East Asian monsoon climate zone (Qu et al., 2004). The interaction between the westerlies and the EASM governs precipitation, water vapor transport, and thus the climate of northwestern China (Feng et al., 2004; Wang et al., 2005; Li et al., 2008; Ma et al., 2011).

To estimate the impact of global change on this interaction, it is crucial to comprehend its historical context. Global atmospheric circulation is likely to change, as is the EASM. Climate change will not only affect the regional climate and regional water resources (Ding et al., 2023); it will affect East Asia (dust storms) and even the rest of the globe. Hence, the study of climate in this region is of great practical and theoretical significance (Chen et al., 2019a; Chen et al., 2019b).

The westerlies and the EASM meet at the northern boundary of the Asian summer monsoon (Huang et al., 2023). In northern China, this boundary runs from west to east, along the eastern section of the Qilian Mountains, the southern foothills of the Helan Mountains, the Daqing Mountains, and the western section of the Daxinganling

Mountains. This is not a static boundary. It fluctuates within a range of 200–700 km (Chen et al., 2018). It is important to understand the history of these fluctuations (Huang et al., 2023).

This can be done using climate records such as lacustrine, eolian, and dendrochronological (Sun et al., 2003; Liu et al., 2005; Li, 2009; Chen et al., 2010; Li et al., 2016; Chen et al., 2019b; Qin et al., 2023). Dendrochronology is one of the best tools for studying paleoclimatic changes, due to its precise dating, high resolution, good continuity and high replication (Zhang et al., 2003; Shao et al., 2010; Yang et al., 2014; Liu et al., 2016).

The climate history of the Baotou area, at the northern edge of the EASM, has been studied at interannual and interdecadal scales for the past 260 years, based on June–August precipitation reconstruction from tree-ring samples from the western Yinshan Mountains (Liu et al., 2001; Liu et al., 2003). Using tree-rings and historical records, Kang and Yang (2015) reconstructed the annual precipitation history of the East Asian monsoon northern fringe zone for the last 530 years. They analyzed spatial variability and possible driving mechanisms using the 400-mm isohyet.

Several May–July precipitation sequences have been reconstructed using ring-width and latewood-width data from Chinese pine (*Pinus tabulaeformis*) growing in the Helan Mountains (Ma et al., 2003; Liu et al., 2004; Chen et al., 2016). Studies of tree-ring carbon and oxygen isotopes from Chinese pine samples have shown that $\delta^{18}O$ values increase with summer precipitation, while $\delta^{13}C$ values decrease (Zhang et al., 2005a; Liu et al., 2008). westerlies have also been shown to affect precipitation in the Helan Mountains (Chen et al., 2010).

Principal component analysis of tree-ring chronologies constructed from data collected at several sites in Gansu suggests that trees at these sites were more influenced by EASM than by westerlies (Chen et al., 2013). These researchers also found that the EASM weakened in 1970s, but recovered in the early 1990s. Tree-ring data allowed the reconstruction of 330 years of PDSI (Palmer Drought Severity Index) values for the Mount Hasi region (at the northern boundary of the summer monsoon zone) (Kang et al., 2012). This study confirmed that radial growth of Chinese pine has declined over

the past three decades, due to the weakening of the EASM. Dendrochronological reconstruction of precipitation in the Mount Changling region (again using Chinese pine) suggested that precipitation in that region mainly depends on the EASM (Chen et al. 2012). Other researchers have assembled tree-ring chronologies from pines growing in the Mount Qilian region and the northern mountains of the Hexi Corridor. Here again precipitation is associated with the EASM. These chronologies have allowed scholars to compile precipitation, temperature, and drought records for the last thousand years (Gou et al., 2015a; Gou et al., 2015b; Zhang et al., 2017).

Most modern researchers studying climate change in the region are mostly carried out on single sample sites (Wang et al., 2004; Liu et al., 2005; Chen et al., 2010; Chen et al., 2016; Li et al., 2016; Liu et al., 2016; Chen et al., 2018). While, there is a dearth of multi-site, regional and long time scale studies on the interaction of the westerlies and the EASM. The research focuses on the interplay area, and investigates the spatiotemporal heterogeneity in climate change and its dominant driving factors, specifically related to the westerlies and East Asia monsoon circulation in Alxa Plateau.

Qinghai spruce (*Picea crassifolia*) is a common tree species in the Helan, Changling and Dongdashan mountain areas around the Alxa Plateau. Using dendrochronological methods, we analyzed the climate response characteristics of spruce radial growth on the above three mountains. Combining the relevant Westerly and East Asia monsoon circulation indices, the driving mechanism of the regional climate change by with the interaction and synergistic roles of two atmospheric circulation systems in the Alxa Plateau was explored. The results will lay a theoretical foundation for the climatic evolution of the region and the desertification control.

2. Material and methods

2.1 Study area

The Alxa Plateau is located in the western part of the Inner Mongolia Autonomous Region and is surrounded by mountains (Fig.1). It consists primarily of three deserts: Tengger, Ulan Buh, and Badan Jaran. It lies south of the Gobi desert. It is the main source of the fierce sandstorms and dust storms that blow toward eastern China and the

Pacific. It has been much affected by climate change; sand- and dust storms have increased, much to the detriment of lands to the east. The Chinese government is doing what it can to establish an environmental defense line there. It is currently the Northern Sand Prevention Belt of the National Two Ecological Barrier and Three Belts Ecological Security Strategy Pattern (Xiao et al., 2017; Xiao et al., 2019).

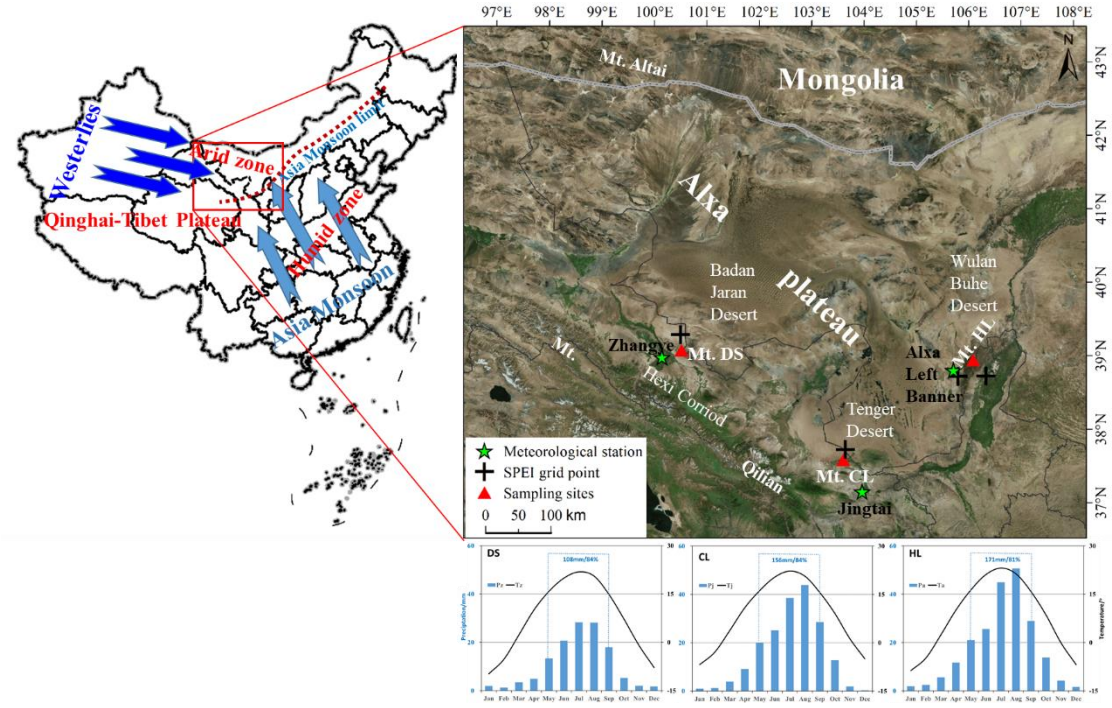

Figure 1. Location of tree-ring sampling sites and climatic diagram of study area (the upper right panel is from Mapworld). Pa/Ta are the monthly total precipitation and monthly mean temperature at the Alxa Left Banner meteorological station (1953–2016); Pj/Tj are the precipitation and temperature figures for the Jingtai meteorological station (1957–2017); Pz/Tz are the precipitation and temperature figures for the Zhangye meteorological station (1957–2017). The dashed box and appended data indicate the total growing season precipitation in the study area and the proportion of total annual precipitation.

There are several mountain ranges surrounding the Alxa Desert, such as the Helan Mountains in the east, the northern mountains of the Hexi Corridor, and the outliers of the Altai Mountains in the north. These mountains not only block the eastward and southward expansion of the desert (driven by high pressure regions from Mongolia);

159 they are also the source of mountain rivers and streams that water the oases on the
160 plateau.
161 The Alxa Plateau is located in the eastern margin of the inland arid region of Central
162 Asia. It is affected not only by the mid-latitude westerly circulation, but also by the
163 Asian monsoon and the Tibet plateau monsoon. It is in the zone where the mid-latitude
164 westerly circulation and the Asian monsoon interact (Xiao et al., 2017; Chen et al.,
165 2019b). As a result, vegetation cover in this region there is characterized by
166 pronounced interannual variability (Ou and Qian, 2006; Tang et al., 2006; Li et al.,
167 2013).
168 The Helan Mountains (38°27′~ 39°30′N, 105°20′~106°41′E) (sampling site
169 henceforth abbreviated as HL), are located at the eastern edge of the Tengger Desert.
170 They stretch more than 200 kilometers from north to south; the main peak is ~3,556 m.
171 The mountain forests are dominated by Qinghai spruce and Chinese pine, juniper,
172 mountain aspen, and elm.
173 Mount Changling (37°12′~37°17′, 102°45′~103°48′E) (sampling site henceforth
174 abbreviated as CL) is an independent mountain protruding northward from the
175 remnants of the eastern Qilian Mountains, it is located at the southern edge of the
176 Tengger Desert; its elevations range from 2100 to 2900 m. The dominant tree species
177 are Qinghai spruce and Chinese pine.
178 Mount Dongdashan (39°00′~39°04′N, 100°45′~100°51′E) (sampling site
179 henceforth abbreviated as DS) is located at the southwestern edge of the Badan Jaran
180 Desert and the middle part of Mount Qilian. It is one of the northern mountains along
181 the Hexi Corridor; that range consists of mountains that vary from 2200 to 2637 m in
182 elevation. Forests are dominated by Qinghai spruce and Qilian juniper.The distances
183 between the CL and HL, CL and DS, and DS and HL sampling sites are approximately
184 250 km, 310 km, and 450 km, respectively.
185 The temperatures of the coldest months recorded at meteorological stations in the
186 Alxa Left Banner (a division of the Alxa League region), Jingtai (a county in Gansu),
187 and Zhangye (a city in Gansu) all occurred in January, ranging from -9.8℃ to -6.8℃.

The hottest months at those stations were in July (21.9 ℃ to 23.1 ℃). These meteorological stations are the closest stations to our three sampling sites (Fig.1).

Precipitation measured at those stations varied widely. The multi-year average of total precipitation from May to September was 171 mm at Alxa Left Banner station, 156 mm at Jingtai station, and 108 mm at Zhangye station. This accounted for more than 80% of the annual precipitation (Fig.1).

2.2 Sample collection, processing and data analysis method

2.2.1 Sample collection, processing and dendrochronology construction

Researchers used standard methods of tree-ring sample collection. One core was drilled from each tree in the sample site. We collected 209 cores in total, from five sampling sites at HL, 48 cores from one sampling site at CL, and 81 cores from two sampling sites at DS. Relevant information of the sampling sites is summarized in Table 1.

Chronologies were constructed using standard dendrochronological methods (Cook, 1985). In order to highlight the high frequency signal, the RES chronology is selected for later climate analysis. We calculated the highly significant correlations ($P < 0.001$) between the chronologies of different points at the HL and DS mountains; a weighting method was used to finally synthesize a chronology for each mountain. Generally, the sub-sample signal strength (SSS) index and the mean series intercorrelation (R_{bar}) are used to evaluate the credibility and quality of the chronologies. The length of the reliable chronology is indicated by the parts of the series with a subsample signal strength (SSS) index > 0.85 (Wigley et al., 1984). Another important statistic is the mean series intercorrelation (R_{bar}), which is the mean correlation coefficient among the ring series and is therefore an indication of the common variance.

2.2.2 Climate data, atmospheric circulation indices and the related Analyzing methods for chronological correlation

Climate data for the study areas HL, CL, and DS were collected from the nearest meteorological stations in Alxa Left Banner, Jingtai and Zhangye, respectively (http://data.cma.cn).

We used SPEI (Standardized Precipitation Evapotranspiration Index) to represent the local drought and wetness conditions, which is widely usedin the dendrochronology studies and considering the effects of potential evapotranspiration, precipitation and time scales (Vicente-Serrano et al., 2010). SPEI data (grid-point resolution $0.5^{o}*0.5^{o}$) was obtained from the grid-point datasets of the National Center for Environmental Predictions-National Center for Atmospheric Research (NCEP-NCAR). Time scales ranged from 1 month to 15 months. The mean values of data from two grid-points closest to the HL sampling site (38.75°N, 105.75°E and 38.75°N, 106.25°E; period 1953–2015) were chosen for subsequent analysis. Grid-point data from one site closest to our CL sampling site (37.75N, 103.75E; period 1951–2015) was used for later analysis. Grid-point data from one site closest to our DS sampling site (39.25°N, 100.75°E; period 1951–2015) was also used. As SPEI datasets are multi-scale, we preprocessed the data to identify and select 11-month scaled SPEI datasets for subsequent analysis.

We took into account the so-called lagging effect (the influence of fall and winter climate factors on the radial growth of trees shows up later in the year) and chose to use temperature, precipitation, and SPEI data from September of the previous year to September of the current year (abbreviated as P9–P12 and C1–C9), as collected at each meteorological station, for our climate response analysis.

The East Asian Summer Monsoon Index (EASMI) (Li and Zeng 2005) represents the activity strength of the EASM. Larger EASMI values indicate a stronger summer monsoon, smaller ones a weaker monsoon. In this study, the EASMI (mean values for June–August in the period 1950–2017) defined by Li and Zeng (2005) was used to study the impact of the EASM on climate change in the study area.

The East Asian Summer Monsoon Index (EASMI) represents the activity strength of the EASM. The East Asian summer monsoon (EASM) index is defined as an area-averaged seasonally (JJA) dynamical normalized seasonality (DNS) at 850 hPa within the East Asian monsoon domain (10°-40°N, 110°-140°E) (Li and Zeng 2005)。Larger EASMI values indicate a stronger summer monsoon, smaller ones a weaker monsoon.

In this study, the EASMI (mean values for June–August in the period 1950–2017) defined by Li and Zeng (2005) was used to study the impact of the EASM on climate change in the study area.

We used the Westerly Circulation Index (WCI annual mean; https://cmdp.ncc-cma.net/cn/index.htm) to represent the strength of the mid-latitude westerlies. The larger the WCI value, the stronger the Eurasian latitudinal circulation; the smaller the value, the weaker the Eurasian latitudinal circulation. WCI data (period 1951–2015) were derived from the Eurasian Latitudinal Circulation Index published by the National Climate Center of the China Meteorological Administration (https://cmdp.ncc-cma.net/cn/index.htm).

Interannual and interdecadal (sliding moving average of 11a) chrono-climatic/-cyclonic index correlation and partial correlation analyses were performed using SPSS 19.0. Based on the characteristics of tree-ring series, the sequences were classified into three groups of low, average and high ring widths using mean ± 1δ (δ: standard deviation) as the classification criterion (with mean ± 2δ as the extreme year). Correlation statistical tests were performed with the corresponding annual circulation indices; similar treatments and analyses were performed for the two major circulation indices.

3. Results and analysis

3.1 Ring-width chronologies and their characteristics

Based on the sampling cores from five sample sites at HL, two sample sites at DS, and one sample site at CL, ring-width residual chronologies were derived for each of the three study areas (Fig. 2). Statistical parameters showed that the three chronologies meet the usual requirements for correctly done dendrochronological studies (Table 1).

Table 1. Statistical characteristics of the sampling sites and the tree-ring chronologies.

Table 1. Statistical characteristics of the sampling sites and the tree-ring chronologies.

Sampling sites	HL(5)	CL(1)	DS(2)
Latitude (°N)	38.52–38.97	37.61	39.04

Longitude (°E)	105.83–106.02	103.71	100.78
Elevation (m)	2200–2750	2490	2650–2700
Cores	209	48	81
Reliable period	1891–2018	1866–2017	1823–2015
MS	0.18–0.37	0.28	0.15–0.33
R_{bar}	0.45–0.61	0.56	0.40–0.60
SNR	22.5–56.1	38.9	25.7–42.5
EPS	0.96–0.98	0.98	0.96–0.98
PC1(%)	17.3–63.0	57.9	43.0–62.5

Reliable period (SSS > 0.85), MS (mean sensitivity), R_{bar} (mean series intercorrelation), SNR (signal to noise ratio), EPS (expressed population signal), and PC1 (variance explained by the first principal component) refer to residual chronologies).

3.2 Climate response characteristics

Correlation analysis comparing a) monthly mean temperature and precipitation at neighboring meteorological stations and b) SPEI at the nearest grid-point showed that, overall, the three residual chronologies were correlated negatively with monthly mean air temperature, positively correlated with monthly precipitation, and positively correlated with SPEI during the growing season (Fig. 3).

HL chronology was correlated negatively with mean temperature mainly in C5–C8 in the growing season, but not to the significant level. It was also positively correlated with precipitation in all months except P12, C1, and C9, reaching significant levels ($P < 0.05$) in P9, C5, and C6. All months were positively correlated with SPEI and reached statistical significance ($P < 0.05$), with C3–C8 showing highly significant correlation levels ($P < 0.01$).

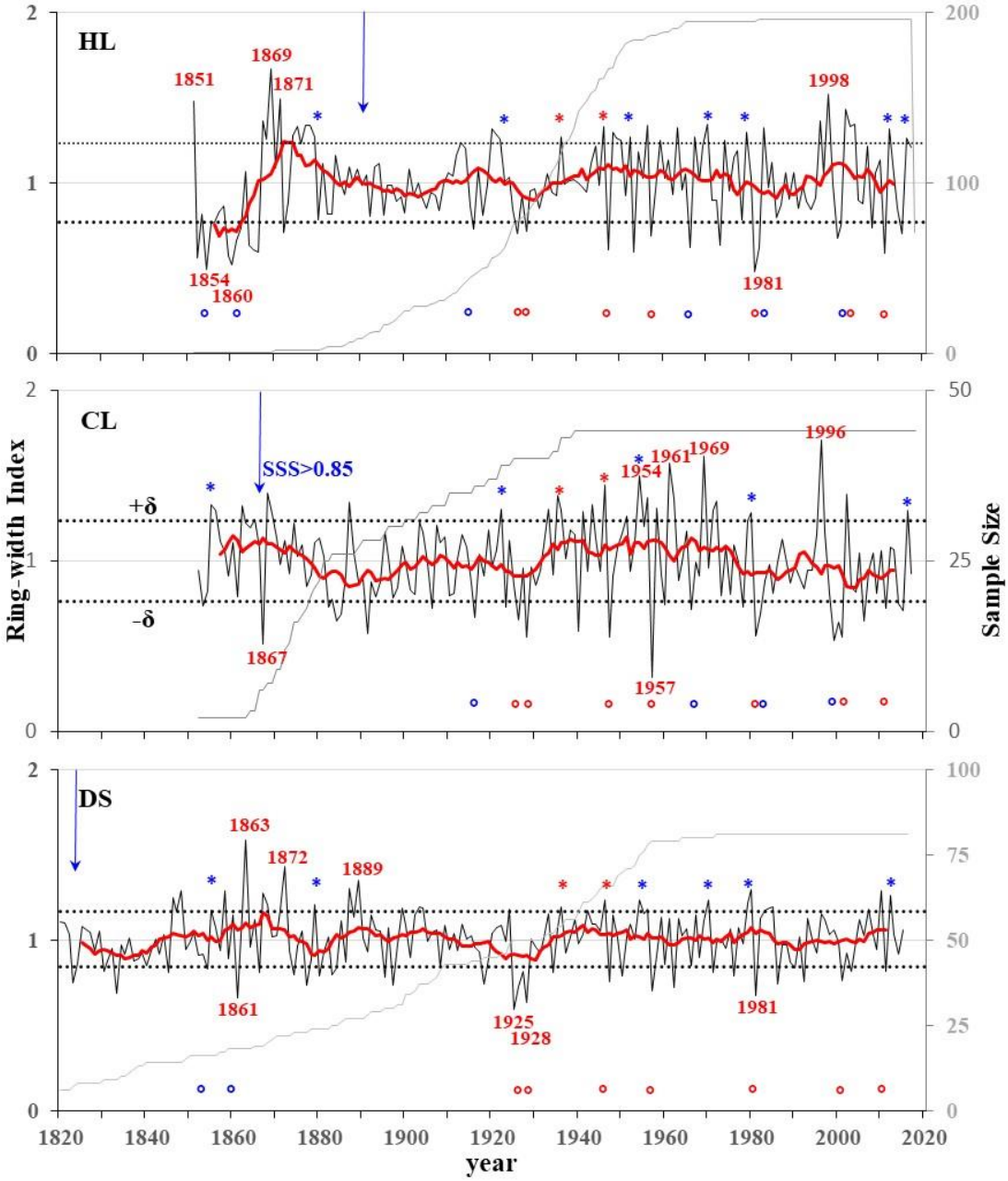

Figure 2. Residual ring-width chronologies for the three study areas. The dark lines indicate the chronology; grey lines indicate the sample depth; red lines indicate the 11-year running mean chronology; dotted horizontal lines indicate the mean value ±1δ; years with data identified as >/< mean ± 2δ (δ: standard deviation); blue * and o indicate the years shared between two of the three sample sites, red * and o shows years shared between three sample sites; blue arrows indicate the start of the reliable residual chronology (SSS > 0.85).

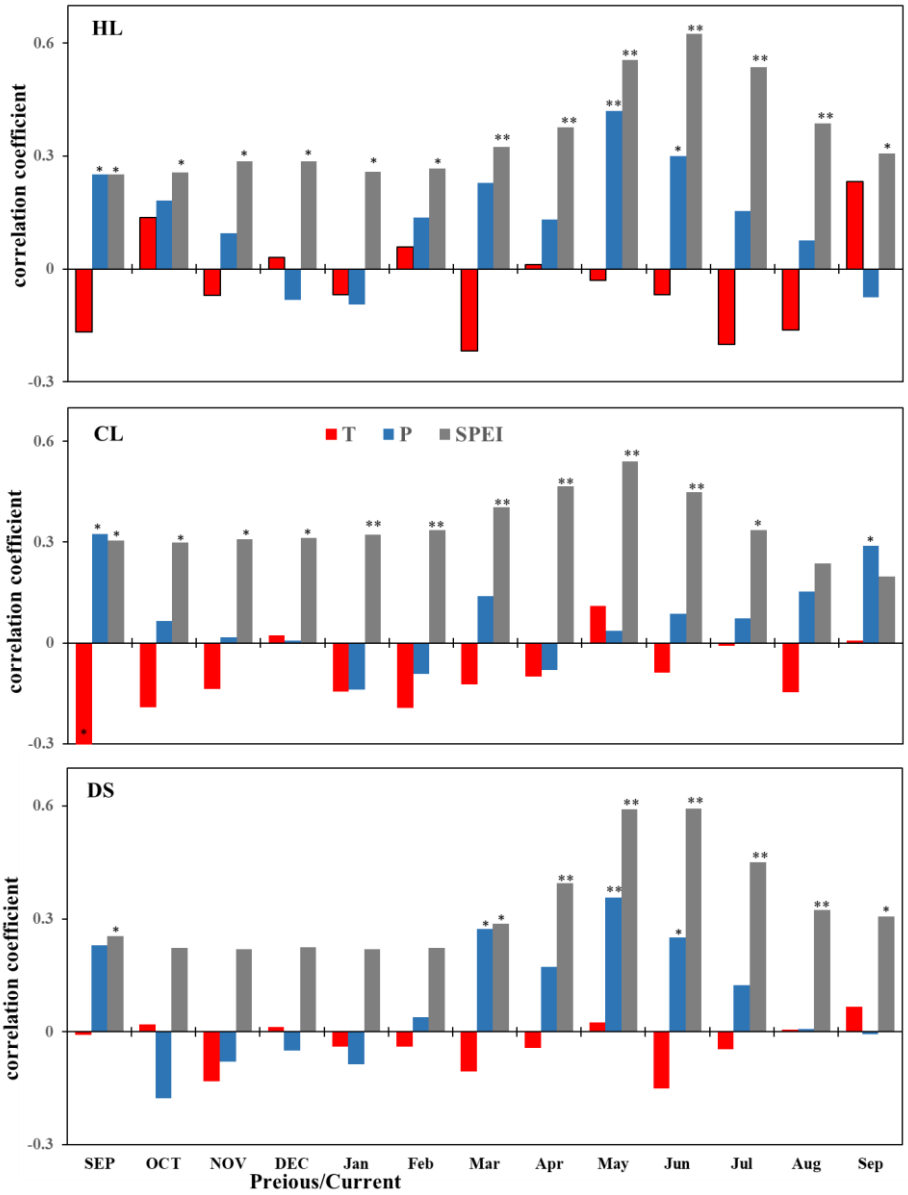

Figure 3. Correlation coefficients (Pearson's r values) between the residual ring-width chronologies of Qinghai spruce at the three study areas (HL, CL and DS) and the observed monthly temperature (T), total monthly precipitation (P), and SPEI. * Pearson's r correlation, significant at $P < 0.05$. * * Pearson's r correlation, significant at $P < 0.01$. Month names of previous year are capitalized.

CL chronology was negatively correlated with the mean temperature in most months, but only reached a significant negative correlation ($P < 0.05$) with P9. CL chronology was positively correlated with monthly precipitation, save for C1, C2, and C4. Only P9 and C9 reached statistical significance ($P < 0.05$). All months were

positively correlated with SPEI, with P9–C7 reaching significant correlation levels ($P < 0.05$) and C1–C7 reaching highly significant correlation levels ($P < 0.01$).

DS chronology showed weak correlations between DS chronology and monthly mean temperatures. None of the correlations reached levels of significance. DS chronology was positively correlated with P9 and C2–C8 precipitation and reached significant correlation levels for C3, C5, and C6 ($P < 0.05$). All months were positively correlated with SPEI, with P9 and C3–C9 reaching significant correlation levels ($P < 0.05$) and C4–C8 reaching highly significant correlation levels ($P < 0.01$).

Overall, the radial growth of Qinghai spruce at the three study areas seems to have been limited, for the most part, by low precipitation during the growing season (April–July). The three chronologies reflect regional wet and dry variations.

3.3 Regional climate changes as recorded by tree-ring widths

3.3.1 Regional climate change viewed at interannual scales

On interannual scales, the three residual chronologies, when compare, showed highly significant correlations (HL–CL: $n = 166$, $r = 0.298$, $P < 0.001$; HL-DS: $n=165$, $r=0.331$, $P < 0.001$; CL–DS: $n = 164$, $r = 0.374$, $P < 0.001$). This indicates that there was a high degree of consistency in the radial growth of Qinghai spruce in the three regions.

According to the results of the chronology-climate response analysis in the previous section, the high and low ring-width indices (mean ± 1~2δ) of the chronology at the three sample sites indicate wetter or drier, and extreme wet or dry years, respectively (Fig. 2).

Overall, the three ring-width residual chronologies (HL, CL, DS) had a total of two shared wetter years and seven shared drier years. The HL and CL chronologies shared four wet years and eleven dry years; the HL and DS chronologies shared five wet years and nine dry years; and the CL and DS chronologies shared five wet years and seven dry years (Fig. 2).

There were no extremely wet years shared by the three sample sites. However, there were two shared wetter years in 1936 and 1946 and several shared wetter years in later years among the three sample sites. For example, note the wetter years in 1922 and 2016 for HL and DS chronologies; 1959, 1979, and 2012 for HL and DS chronologies; 1855, 1954, and 1980 for CL and DS chronologies (Fig. 2).

The extreme drought years are consistent among the three sample sites. For instance, there was an extreme drought year in 1981 at HL and DS sample sites; it was also a drought year at CL. An extreme drought year at CL in 1957 was also a drought year for the other two chronologies. Moreover, the extreme drought year of 1928 at DS was a drought year at the other two sites. Drought years in 1926, 1947, 2001, and 2011 were seen in all three sites and in two of the three sample sites (1916, 1966, 1982, and 2000 at HL and CL; 1854 and 1861 at HL and DS) (Fig. 2).

3.3.2 Characteristics of regional climate change at inter-decadal scales

On the decadal scale, the 11a running mean series indicates that at the HL site there were four wetter periods (mid-1860s to early 1880s; 1910s to 1920s; mid-1930s to mid-1970s; and late 1990s to early 2010s). Four drought periods were seen (mid-1850s to mid-1860s; early 1890s to late 1900s; circa 1930s; and mid-1970s to 1980s) (Fig.4).

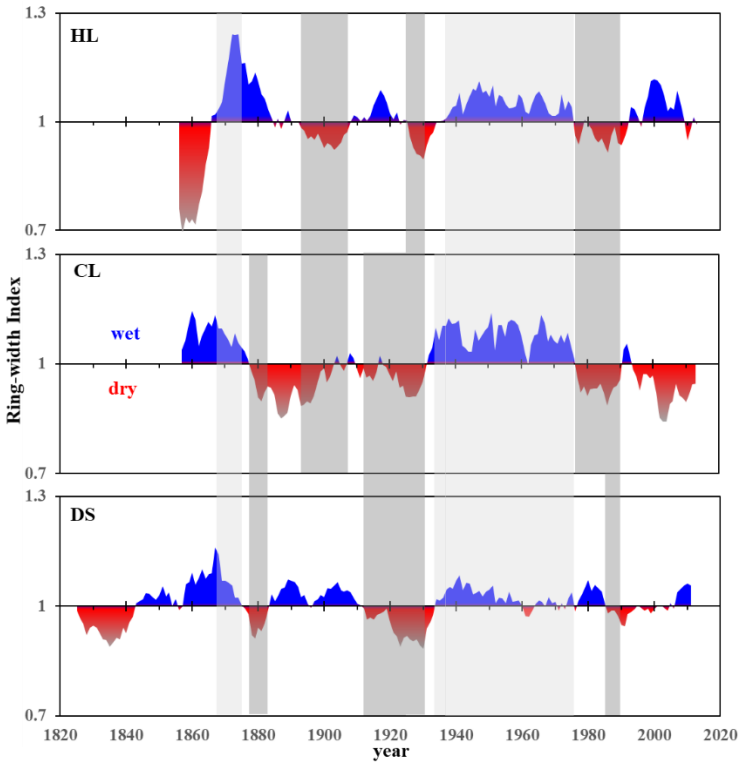

Figure 4. Three regional chronologies demonstrating alternation between dry (red) and wet (blue) years on interdecadal scales (11 a running mean). The gray and light gray bands indicate consistent changes of the dry and wet periods.

The CL regional chronology revealed two main wetter periods (mid-1850s to mid-1870s; mid-1930s to mid-1970s) and two longer drought periods (late 1870s to early 1930s; following the late 1970s) (Fig.4).

The DS regional chronology showed four main wetter periods (mid-1840s to mid-1870s; mid-1880s to late 1900s; mid-1930s to mid-1980s; and late 2000s to early 2010s). There were four drought periods (mid-1820s to mid-1840s; mid-1870s to 1880s; early 1910s to early 1930s; and late 1980s to mid-2000s). The drought during the last drought period was less severe (Fig.4).

The three chronologies show both synchronized phases and differential changes on an interdecadal scale. The more synchronized dry phases of climate change were the drought periods of the 1930s and 1990s. When we compared the DS chronology to the HL and CL chronologies on decadal scales, we noted that DS droughts tended to last

longer and that they started and ended later than CL droughts. However, HL and DS droughts tended to end at the same time (Fig.4).

There were two wet periods in 1870s and the mid-1930s to 1970s which were shared by all three sample sites. The latter period was the longest lasting wet period we saw in our study. There were also dry and wet periods that were not shared by any of our sites. There was an HL drought (mid-1850s to mid-1860s) which was not shared by the other two sites, which were wetter. HL and CL shared drought periods (1890s to 1910s; 1980s) while DS was wetter. Conversely wetter periods at HL were sometimes accompanied by drought in the other two sites. Drought at CL was sometimes accompanied by wet periods at the other two sites. DS was wet during the 2010s but the other two sites were in drought (Fig.4).

The results of the above studies show that there are diversified and complex features in the interdecadal processes of climate change in different regions around the Alxa Plateau.

3.4 Driving mechanism of the regional climate changes

3.4.1 Driving mechanism of the regional climate changes of typical years

On the interannual scales, three regional chronologies we developed showed fairly weak negative correlations between the EASM and the westerlies; none of the correlations were statistically significant. We carried out correlation analyses of the three regional ring-width chronologies and two major circulation indices. This was done in high, medium and low ring-width index groups (Fig. 5; 6).

At HL, the results of our combined subgroup correlation analyses suggest that correlations between radial growth groups and atmospheric circulations were stable. Correlation between the higher ring-width group and atmosphere circulation indices and between the lower ring-width group and the WCI were all significant ($P < 0.05$) (Fig. 5; 6).

At CL, correlations between the higher and middle ring-width groups to the WCI and the higher and middle WCI groups to the ring-width index were all negative. Correlations between the higher and middle ring-width groups and the EASMI, and

between the higher and middle EASMI groups with the ring-width index were inconsistent (Fig. 5; 6).

At DS, correlations between the higher and lower ring-width groups and the EASMI, and between the higher and lower EASMI groups to the ring-width indices, were consistent. The correlations between the higher ring-width groups and the WCI, and between the higher WCI groups and the ring-width index were consistent. However, the correlations between the lower ring-width groups and the WCI, also between the lower WCI groups and the ring-width index, were inconsistent (Fig. 5; 6).

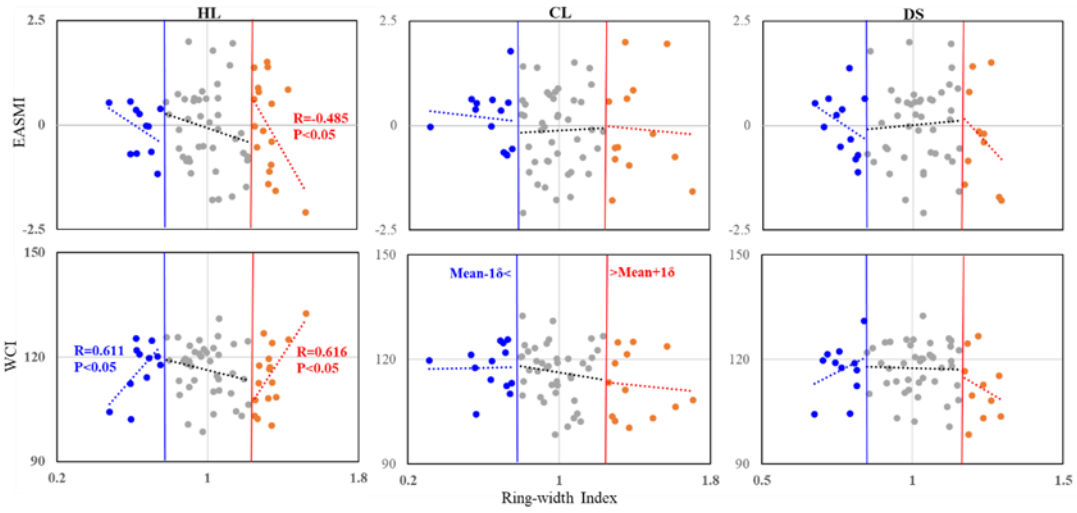

Figure 5. Grouping related charts among the ring-width index of three regions (HL, CL and DS) and the two atmospheric circulations' indices (EASMI and WCI), grouped by chronological values. The noted numbers are the person correlation coefficients (two-tails test) and the corresponding significant credible level. Only the significant correlations were labeled. Red dots indicate the higher ring-width index group (> mean+1δ), gray dots indicate the middle ring-width index group (> mean-1δ ~< mean+1δ), and blue dots indicate the lower ring-width index group (> mean-1δ).

Except for HL, none of the ring-width groups or the atmospheric circulation index groups of the others reached a level of significance. These results suggest that HL is strongly affected by size of, and the interaction between, the EASM and the Westerly winds. On an interannual scale, stronger west winds and a weaker monsoon could result in variations from the ordinary climate (veering towards drier or wetter). Weaker west

winds and a stronger monsoon formed the normal climate at HL. At the CL and DS sites, both atmospheric circulations were relatively weak on interannual scales. They had complex interactions.

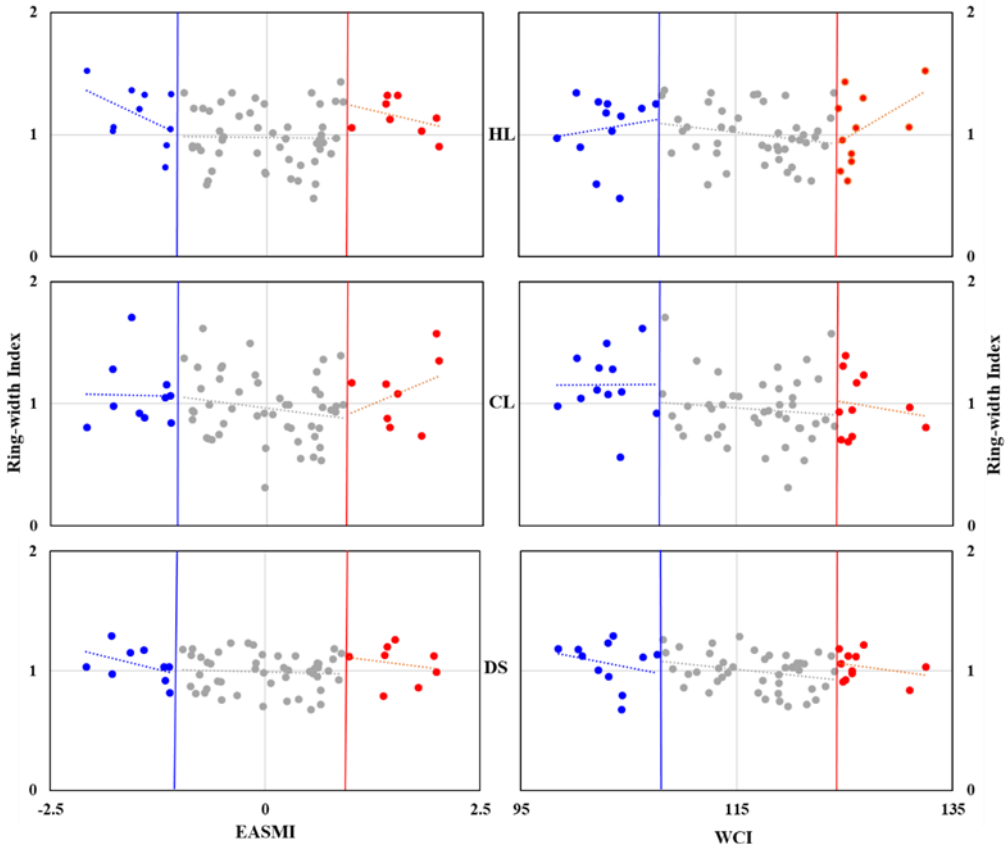

Figure 6. Grouping related charts among the two atmosphere circulations' index (EASMI and WCI) and the ring-width index of three regions (HL, CL, and DS), grouped by the two atmosphere circulations' index. Red dots indicate the higher atmosphere circulations' index group (> mean+1δ), gray dots indicate the middle atmosphere circulations' index group (> mean-1δ ~< mean+1δ), and blue dots indicate the lower atmosphere circulations' index group (> mean-1δ).

3.4.2 Driving mechanisms of the regional climate changes on a decadal scale

At HL, both the EASM and the westerly circulation had highly significant effects on the radial growth of the Qinghai spruce. At CL, the EASM also had highly significant effects on radial growth of the Qinghai spruce. There, correlation coefficients were higher for the EASMI (EASM index) than they were for the HL index. Correlations between the WCI and radial growth were negative, but not at a significant level.

At DS, correlation between radial growth and the WCI was extremely negative ($P < 0.01$). Correlation between radial growth and the EASM was positive ($P > 0.1$) (Fig. 7). These results suggest that at HL, alternations between dry and wet seasons were affected both by the EASM and the westerlies. If either of the two atmospheric circulations was stronger, the climate tended to be wetter. At CL, alternations between dry and wet were affected mainly by the EASM. When the EASM was stronger, the climate was wetter. At DS, the climate was affected mainly by the westerlies. The stronger the winds, the wetter the climate (Fig. 7).

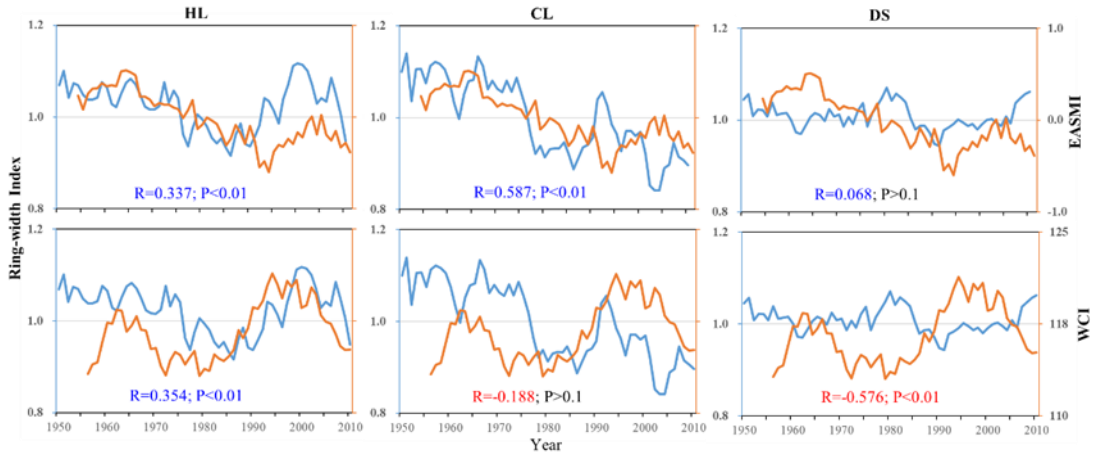

Figure 7. Interdecadal scale (11-a running average) correlations of the three residual chronologies with the EASMI and WCI.

The results of our interdecadal partial correlation analysis of the three RES-chronologies with the WCI and EASMI further illustrate the impacts of the two circulation systems on the climate of the three regions (Table 2).

At HL, if we control one variable (the WCI or EASMI) from our analysis, the other variable will all showed a positive correlation with its chronology ($P < 0.0001$). At CL, if we controlled the WCI, we find a positive significant correction between the chronology and EASMI ($P < 0.0001$). If we controlled the effect of EASMI, we saw a weak negative correction between the chronology and WCI (Table 2). At DS, if we controlled EASMI, we saw a negative significant correlation between the chronology and WCI ($P < 0.0001$). If we controlled the WCI, we saw an insignificant negative correlation between the chronology and EASMI (Table 2).

Table 2. Inter-decadal partial correlation analysis of the three residual-chronologies with the WCI and EASMI.

	HL	CL	DS
WCI	0.489 ***	0.550***	-0.172
EASMI	0.511***	-0.001	-0.591***

Correlation significance levels (two-tailed test): *** $P < 0.001$.

Summary: at HL (on the eastern boundary of the Alxa Plateau), both EASMI and WCI influenced the alternation between wet and dry; at CL (on the southern boundary of the Alxa Plateau), climate was mainly influenced by the EASM. At DS (on the western boundary of the Alxa Plateau and the middle part of Hexi Corridor), climate was mainly influenced by the westerlies.

4. Discussion and conclusions

4.1 Climate changes indicated by regional chronologies

Our chronology-climate response analysis (Fig. 3) showed that the radial growth index of Qinghai spruce in the HL, CL and DS mountains were a good record of regional climate changes around the Alxa Plateau (Fig. 2). On the interannual scale, the three regional chronologies noted that the extreme drought years of 1928, 1957 and 1981 were shared by two or more locations, as were the drought years of 1854, 1861, 1916, 1926, 1947, 1966, and 2001 (Fig. 2).

We note that drought was also reported by other tree-ring studies for these regions (Chen et al., 2016), also for the Qilian Mountains (Zhang et al., 2011; Zhang et al., 2017). Several other drought years (1854, 1884, and 1925–1928) were also seen in the dry-wet climate history (PDSI and recorded by tree-ring-widths) in the nearby area of Mount Hasi, which lies on the edge of the regions most influenced by the EASM (Kang et al., 2012).

The drought years of 1823, 1833, 1854, 1877, 1883–1885, 1895, 1908, 1971, 1992, and 2003 seen in results for the Alxa Plateau are also seen in twelve tree-ring reconstructed drought series for the Qilian Mountains (an area mainly influenced by westerlies) (Zhang et al., 2011). We also note that wetter years seen in our three regional

chronologies were also seen in results from the Hasi and Xinglong Mountains, which are also on the edge of the area influenced by the EASM) (Fang et al., 2009; Kang et al., 2012).

If we compare our results with those seen for the EASM-affected areas at Mount Guiqing, 1820–2005 (Fang et al., 2010), we noted that only three of the eight drought years in that area (1928, 2000, and 2001) were seen in our three chronologies. We also noted results from the westerly-influenced area at Mount Tianshan (Jiang et al., 2017). The wetter years of 1846, 1903 and 1942 at DS were also extreme wet years at Mount Tianshan. Two wet years, 1848 and 1959, recorded at DS are either one year earlier or one year later than extremely wet years at Mount Tianshan, which might suggest some correlation. Drier years at DS (1884, 1947 and 1951) are one or two years later than the extremely dry years at Mount Tianshan. This suggests that these phenomena could be related to broader changes in the extent and strength of the atmospheric circulation.

On a broader (interdecadal) scale, an extreme drought period in 1920s–1930s was shared by much of northern China (Liang et al., 2006; Fang et al., 2009; Fang et al., 2010). This is the same drought that we note our chronologies for HL, CL and DS (Liu et al., 2002; Chen et al., 2010; Fan et al., 2012; Liu et al., 2013; Zhang et al., 2015). A drought in 1890–1900 was noted by dendrochronological studies and regional history documents (Yuan, 1994; Ma et al., 2003; Cai and Liu, 2007).

Ma and Fu's (2006) study showed a broad shift towards a drying climate in 1977–78 (eastern area in northwestern China, also northern China). Several other dendrochronological studies showed a combination of high temperatures and low precipitation in the late 1970s to early 1990s (Zhang et al., 2005b; Cai and Liu, 2007; Cai, 2009). This same drought was seen at DS, if somewhat later and for a shorter time. We also noted its effects at HL and CL. This would be consistent with the increased humidity of the climate in the eastern region of Northwest China (the EASM-influenced region experiencing > 400 mm precipitation). This region would include Mount Xinglong (Fang et al., 2009; Chen et al. 2015), the easternmost part of the Qilian Mountains, and Mount Guiqing (Fang et al., 2010).

519 The wet period that lasted from the 1940s to the early 1970s has been recorded by
520 several tree-ring-width chronologies covering HL, CL, and DS (Liu et al., 2004; Liu et
521 al., 2005; Gao et al., 2006; Cai, 2009; Chen et al., 2010). Regional history documents
522 also record some severe floods disasters in this period (Yuan, 1994). We also see this
523 wet period in tree-ring-width chronologies from Mount Xinglong (Fang et al., 2009;
524 Chen et al. 2015) and Mount Guiqing (Fang et al., 2010).
525 The wet period in the 1830s–1840s evident in the chronologies in Xinglong
526 Mountain (Fang et al., 2009) (Chen et al. 2015) and Guiqing Mountain (Fang et al.,
527 2010) corresponds to the dry period of DS. The wet period in the 1830s–1840s
528 corresponds to the dry period of HL and CL, and to the wet period of DS. The observed
529 phenomena can be attributed to differences in the extent and intensity of EASM and
530 westerly atmospheric circulations.
531
532 **4.2 Influence of atmospheric circulations and their interaction on climate change**
533 **in the Alxa Plateau**
534 Water vapor carried by the westerlies will extend southward to the northern part of
535 Qinghai, the Hexi region of Gansu, the northern part of Ningxia, and the northern part
536 of Shaanxi Province, sometimes passing through the northern border of the Xinjiang
537 region (Li et al., 2012). The area bounded by 35° and 55°N, and 110°E and 140°E seems
538 to be crucial to fluctuations in the westerlies. This in turn affects the distribution of rain
539 belts in summer. Its mean WCI are weaker positively to the rainfall in the middle of
540 Yellow River Basin and its northern regions (Yan et al., 2007). The results showed that
541 the middle ring-width index group of Qinghai spruce in the three sample sites, which
542 are located in the key area for interaction between wind and monsoon, presented weaker
543 negative correlation with WCI on the interannual scale (Fig. 5).
544 The EASM boundary zone has a greater influence on precipitation at higher
545 latitudes and thus on vegetation growth. This boundary zone can fluctuate due to the
546 interannual variability of the EASM and the westerlies. There may be lagging effects
547 at the mid-latitudes (Ou and Qian, 2006). Again, we note that on an interannual scale,

there is much variation in the strengths and interactions of the EASM and westerly circulation and thus on climate in our three study regions (Fig. 5).

Sun et al. (2019) showed that when the westerly circulation strengthens, high latitude air pressure drops across the entire Asian continent. Siberian high pressures and the EASM are weakened. The southward movement of the cold air is also correspondingly weakened. That is not conducive to the north and south of the cold and warm air vapor exchange to form precipitation. When the lower of the WCI and weakened latitudinal circulation, the meridional circulation will strengthen, which favors the exchange of warm and cold air between the north and south to form precipitation.

Yang et al. (2019) proposed that in years with weak summer westerlies in the middle latitudes, the upper-level jet stream tends to shift southward. This southward displacement of the jet stream, coupled with weakened lower-level divergence, hampers the northward transport of warm air into the southwestern region. Consequently, this leads to reduced availability of water vapor sources and ultimately results in diminished summer precipitation within the transitional zone of typical monsoon activity. If the jet stream moves northward, precipitation increases.

Xu et al. (2010) indicated that in the middle Qilian Mountains the westerlies affect precipitation directly, while the EASM only indirectly affects precipitation. When the westerlies become stronger (weaker), the high precipitation zone moves northwestward (southeastward).

At DS, radial growth showed weak negative correlations with higher WCI and also higher, middle, and lower EASMI groups (Figs. 5; 6). At HL, when high chronology indices are positive they are significantly correlated with westerly circulation; when they are negative they significantly correlate with EASM (Figs. 5; 6). At CL, which lies further to the south than HL, a higher EASMI leads to a more humid climate. Other effects are more complicated: for example, the higher and lower ring-width index groups, associated with extreme dry and wet climate years, have weak negative correlations to EASMI (Figs. 5; 6). Jiang et al. (2019) published the results of their hydrogen and oxygen isotope studies of surface water at more than 3,000 sampling sites

in northern China. They showed that surface water recharge in the DS Mountains is due to the westerlies; recharge in the CL Mountains is due to the EASM. The HL Mountains, in contrast, sit at the boundary of the EASM; water recharge there is due to both the EASM and the westerlies.

Jiang and Wang (2005) notes significant declines in the EASM in the mid-1960s and mid-1970s, which led to decline in the radial growth of Qinghai spruce in our study area. The effect of the latter declined period was much greater than that of the former, whatever the intensity or duration. The effects of these declines were stronger at CL and DS than at HL. In the mid-1970s, EASM retreat had stronger negative effects at CL and then at HL. However, decline in the EASM proved to be a facilitator of radial growth at DS (Fig. 7).

In the same period the westerly circulation also retreated. The EASM retreated again in 1990s, while the westerlies strengthened. This resulted in a drier climate in the CL Mountains. However, it was also correlated with fluctuating wet periods at HL and a weak wet period at DS. The above results, to a certain extent, support our view on the driving mechanisms of climate change in the three study areas, especially in the DS Mountains.

When we look at this area on a geologic scale, we learn that the westerly circulation strengthened during the Ice Age. Westerly jet streams moved southward to about 35^{o}N. When the westerlies weakened in the Interglacial Age, the westerly jet streams moved northward to ~37^{o}N (Sun et al., 2003). A study of Holocene lake level evolution in the ancient Zhuye lake, central Alxa Plateau, showed that lake-level change was subject to the combined effects of EASM and the arid climate of Central Asia (Li, 2009). This result further illustrates the complexity of lake evolution and climate change in the EASM marginal zone.

The westerly circulation also interacts with the monsoon on the Tibetan Plateau, which has a profound effect on the climate of the Asian monsoon region as well as the global climate (Qu et al., 2004). There has also been much research using proxy indicator cycles indicating that our study area is also influenced by large-scale ocean-atmosphere changes on interannual and interdecadal scales, such as the North Atlantic

Oscillation (NAO), Pacific Decadal Oscillation (PDO), El Niño-Southern Oscillation (ENSO), and sunspot activity (Gou et al., 2015a; 2015b; Liu et al., 2016; Wang et al., 2017). Generally, the intensity of ENSO was inversely correlated with the intensity of the EASM. There was a negative correlation between PDO and regional dry-wet variation in the west of 100° E. When the NAO is in positive phase (negative phase), it indicates that the mid-latitude westerly winds are in strong (declining) phase, which is conducive to (unfavorable) precipitation formation.

However, all of the above-mentioned large-scale climate and ocean-atmosphere changes affect the EASM and westerly circulation through different pathways (Li. 2009), which in turn have various effects on the northwestern edge zone of the EASM and the zone of interaction between the two major atmospheric circulations.

In conclusion, based on the analysis of the regional chronologies collected in the HL, CL and DS mountains that are arrayed around the Alxa Plateau, we can safely assert that the radial growth of Qinghai spruce in the study area is mainly affected by regional precipitation. This precipitation varies constantly over time and space, primarily influenced by the interactions between two atmospheric circulation systems, EASM and westerlies. At HL, both of these atmospheric circulation systems play a significant role in shaping climate changes. At CL, the climate is mainly influenced by the EASM. At DS, climate is more heavily influenced by the westerly circulation.

In the future, it is to be hoped that more refined, smaller scale research can be done on the climate history in the deserts of the Alxa Plateau. Such research may finally to provide a theoretical basis to explain regional climate driving mechanisms and thus enable better desertification controls.

Data availability

All data for this paper is available upon request.

Author contributions

All authors approved the manuscript and agreed on its submission. Shengchun Xiao: Conceptualization, Methodology, Funding acquisition, Investigation, Resources,

Writing - Original Draft, Writing review and editing. Xiaomei Peng: Funding acquisition, Writing review. Quanyan Tian: Investigation, Data collection and procession. Aijun Ding: Investigation, Data collection and procession. Jiali Xie: Methodology and Writing review. Jingrong Su: Methodology and Writing review.

Competing interests

The contact author has declared that none of the authors has any competing interests.

Acknowledgements

The study was jointly funded by the National Natural Science Foundation of China (NSFC) (No.42171031; 42171167); Inner Mongolia Autonomous Region Special Fund project for transformation of Scientific and technological Achievements (2021CG0046).

References

Cai, Q. F.: Response of *Pinus tabulaeformis* tree-ring growth to three moisture indices and January to July Walter index reconstruction in Helan mountain, Marine geology & Quaternary geology, 29, 131–136 (In Chinese with English abstract), https://doi.org/10.3724/SP.J.1140.2009.06131, 2009.

Cai, Q. F. and Liu, Y.: January to August temperature variability since 1776 inferred from tree-ring width of *Pinus tabulaeformis* in Helan Mountain, Journal of Geographical Sciences, 17, 293–303, https://doi.org/10.1007/s11442-007-0293-5, 2007.

Chen, F., Yuan, Y. J., Zhang, T. W., and Linderholm, H. W.: Annual precipitation variation for the southern edge of the Gobi Desert (China) inferred from tree rings: linkages to climatic warming of twentieth century, Nat. Hazards, 81, 939–955, https://doi.org/10.1007/s11069-015-2113-z, 2016.

Chen, F., Wei, W. S., Yuan, Y. J., Yu, S. L., Shang, H. M., Zhang, T. W., Zhang, R. B., Wang, H. Q., and Qin, L.: Variation of annual precipitation during 1768-2006 in Gansu Inferred from multi-site tree-ring chronologies, Journal of Desert Research, 33, 1520–1526 (In Chinese with English abstract), https://doi.org/10.7522/j.issn.1000-694X.2013.00218., 2013.

Chen, F., Yuan, Y. J., Wei, W. S., Yu, S. L., Fan, Z. A., Zhang, R. B., Zhang, T. W., Li, Q., and Shang, H. M.: Temperature reconstruction from tree-ring maximum latewood density of Qinghai spruce in middle Hexi Corridor, China, Theoretical and Applied Climatology, 107, 633–643, https://doi.org/10.1007/s00704-011-0512-y, 2012.

Chen, F., Yuan, Y. J., Wei, W. S., Yu, S. L., Li, Y., Zhang, R., Fan, Z., Zhang, T., and Shang, H.:

PDSI changes of May to July recorded by tree rings in the northern Helan Mountains, Advance in Climate Changes Research, 65, 344-348 (In Chinese with English abstract), 2010.

Chen, F. H., Chen, J. H., Huang, W., Chen, S. Q., Huang, X. Z., Jin, L. Y., Jia, J., Zhang, X. J., An, C., and Zhang, J.: Westerlies Asia and monsoonal Asia: spatiotemporal differences in climate change and possible mechanisms on decadal to sub-orbital timescales, Earth-Sci. Rev., 192, 337–354, https://doi.org/10.1016/j.earscirev.2019.03.005, 2019a.

Chen, F. H., Fu, B. J., Xia, J., Wu, D., Wu, S. H., Zhang, Y. L., Sun, H., Liu, Y., Fang, X. M., Qin, B. Q., Li, X., Zhang, T. J., Liu, B. Y., Dong, Z. B., Hou, S. G., Tian, L. D., Xu, B. Q., Dong, G. H., Zheng, J. Y., Yang, W., Wang, X., Li, Z. J., Wang, F., Hu, Z. B., Wang, J., Liu, J. B., Chen, J. H., Huang, W., Hou, J. Z., Cai, Q. F., Long, H., Jiang, M., Hu, Y. X., Feng, X. M., Mo, X. G., Yang, X. Y., Zhang, D. J., Wang, X. H., Yin, Y. H., and Liu, X. C.: Major advances in studies of the physical geography and living environment of China during the past 70 years and future prospects, Science China Earth Sciences, 62, 1665–1701, https://doi.org/10.1007/s11430-019-9522-7, 2019b.

Chen, J., Huang, W., Jin, L., Chen, J. H., Chen, S. Q., and Chen, F. H.: A climatological northern boundary index for the East Asian summer monsoon and its interannual variability, Science China Earth Sciences, 61, 13–22, https://doi.org/10.1007/s11430-017-9122-x, 2018.

Cook E.R.: A Time Series Analysis approach to tree ring standardization (Dendrochronology, forestry, dendroclimatology, autoregressive process)[D]. Tuscon, Arizona: The University of Arizona, 1985.

Ding, Y. H., Liu, Y. J., Xu, Y., Wu, P., Xue, T., Wang, J., Shi, Y., Zhang, Y. X., Song, Y. F., and Wang, P. L.: Regional responses to global climate change: progress and prospects for trend, causes, and projection of climatic warming-wetting in Northwest China, Advances in Earth Science, 38, 551–562 (In Chinese with English abstract), https://doi.org/10.11867/j.issn.1001-8166.2023.027, 2023.

Fan, Z. A., Wei, W. S., Chen, F., and Yuan, Y. J.: Precipitation variation from 1775 to 2005 at the eastern margin of Tengger Desert, China inferred from tree-ring, Journal of Desert Research, 32, 996–1002 (In Chinese with English abstract), 2012.

Fang, K. Y., Gou, X. H., Chen, F. H., D'arrigo, R., and Li, J. B.: Tree-ring based drought reconstruction for the Guiqing Mountain (China): linkages to the Indian and Pacific Oceans, Int. J. Climatol., 30, 1137–1145, https://doi.org/10.1002/joc.1974, 2010.

Fang, K. Y., Gou, X. H., Chen, F. H., Yang, M. X., Li, J. B., He, M. S., Zhang, Y., Tian, Q. H., and Peng, J. F.: Drought variations in the eastern part of northwest China over the past two centuries: evidence from tree rings, Clim. Res., 38, 129–135, https://doi.org/10.3354/cr00781, 2009.

Feng, W., Wang, K. L., and Jiang, H.: Influences of westerly wind inter-annual change on water vapor transport over northwest china summer, Plateau Meteorology, 23, 270–275 (In Chinese with English abstract), 2004.

Gao, S. Y., Lu, R. J., Qiang, M. R., Ha, S., Zhang, D. S., Chen, Y., and Xia, H.: Precipitation variation recorded by tree-rings in the northern Tengger Desert of the last 140 years, Chin. Sci. Bull., 51, 326–331, https://doi.org/10.1360/csb2006-51-3-326, 2006.

Gou, X. H., Gao, L. L., Deng, Y., Chen, F. H., Yang, M. X., and Still, C.: An 850‐year tree‐ring‐based reconstruction of drought history in the western Qilian Mountains of northwestern China, Int. J. Climatol., 35, 3308–3319, https://doi.org/10.1002/joc.4208, 2015a.

Gou, X. H., Deng, Y., Gao, L. L., Chen, F. H., Cook, E., Yang, M. M., and Zhang, F.: Millennium tree-ring reconstruction of drought variability in the eastern Qilian Mountains, northwest China, Climate Dynamics, 45, 1761–1770, https://doi.org/10.1007/s00382-014-2431-y, 2015b.

Huang, L. X., Chen, J., Yang, K., Yang, Y. J., Huang, W., Zhang, X., and Chen, F. H.: The northern boundary of the Asian summer monsoon and division of westerlies and monsoon regimes over the Tibetan Plateau in present-day, Science China Earth Sciences, 66, 882–893, https://doi.org/10.1007/s11430-022-1086-1, 2023.

Jiang, D. B. and Wang, H. J.: Natural interdecadal weakening of East Asian summer monsoon in the late 20th century, Chin. Sci. Bull., 50, 1923–1929, https://doi.org/10.1360/982005-36, 2005.

Jiang, P., Liu, H. Y., Wu, X. C., and Wang, H. Y.: Tree-ring-based SPEI reconstruction in central Tianshan Mountains of China since A.D. 1820 and links to westerly circulation, Int. J. Climatol., 37, 2863–2872, https://doi.org/10.1002/joc.4884, 2017.

Jiang, W. J., Wang, G. C., Sheng, Y. Z., Shi, Z. M., and Zhang, H.: Isotopes in groundwater (^{2}H, ^{18}O, ^{14}C) revealed the climate and groundwater recharge in the Northern China, Sci. Total Environ., 666, 298–307, https://doi.org/10.1016/j.scitotenv.2019.02.245, 2019.

Kang, S. Y. and Yang, B.: Precipitation variability at the northern fringe of the Asian summer monsoon in Northern China and its possible mechanism over the past 530 years, Quaternary Sciences, 35, 1185–1193, https://doi.org/10.11928/j.issn.1001-7410.2015.05.14, 2015.

Kang, S. Y., Yang, B., and Qin, C.: Recent tree-growth reduction in north central China as a combined result of a weakened monsoon and atmospheric oscillations, Clim. Change, 115, 519–536, https://doi.org/10.1007/s10584-012-0440-6, 2012.

Li, D. L., Shao, P. C., and Wang, H.: The position variations of the north boundary of East Asia subtropical summer monsoon in 1951-2009, Journal of Desert Research, 33, 1511–1519 (In Chinese with English abstract), https://doi.org/10.7522/j.issn.1000-694X.2013.00217, 2013.

Li, J. L., Li, Z. R., Yang, J. C., Shi, Y. Z., and Fu, J.: Analyses on spatial distribution and temporal variation of atmosphere water vapor over northwest China in summer of later 10 years, Plateau Meteorology, 31, 1574–1581 (In Chinese with English abstract), 2012.

Li, J. P. and Zeng, Q. C.: A new monsoon index, its interauual variability and related with

monsoon precipitation, Climatic and Environmental Research, 10, 351–365 (In Chinese with English abstract), 2005.

Li, W. L., Wang, K. L., Fu, S. M., and Jiang, H.: The interrelationship between regional Westerly index and the water vapor budget in Northwest China, Journal of Glaciology and Geocryology, 30, 28–34 (In Chinese with English abstract), 2008.

Li, Y.: The pollen records from lake sediments and climate & lake model in the Marginal area of Asian monsoon, Lanzhou University, Lanzhou, China, 2009.

Li, Z. X., Feng, Q., Song, Y., Wang, Q. J., Yang, J., Li, Y. G., Li, J. G., and Guo, X. Y.: Stable isotope composition of precipitation in the south and north slopes of Wushaoling Mountain, northwestern China, Atmospheric Research, 182, 87–101, https://doi.org/10.1016/j.atmosres.2016.07.023, 2016.

Liang, E. Y., Liu, X. H., Yuan, Y. J., Qin, N. S., Fang, X. Q., Huang, L., Zhu, H. F., Wang, L., and Shao, X. M.: The 1920s drought recorded by tree rings and historical documents in the semi-arid and arid areas of Northern China, Clim. Change, 79, 403–432, https://doi.org/10.1007/s10584-006-9082-x, 2006.

Liu, J. B., Chen, J., Chen, S. Q., Yan, X. W., Dong, H. R., and Chen, F. H.: Dust storms in northern China and their significance for the concept of the Anthropocene, Science China Earth Sciences, 65, 921–933, https://doi.org/10.1007/s11430-021-9889-8, 2022.

Liu, Y., Cai, Q. F., Ma, L. M., and An, Z. S.: Tree ring precipitation records from Baotou and the East Asia summer monsoon variations for the last 254 years, Earth Sci. Front., 8, 91–97 (In Chinese with English abstract), https://doi.org/10.3321/j.issn:1005-2321.2001.01.012, 2001.

Liu, Y., Sun, C. F., Li, Q., and Cai, Q. F.: A *Picea crassifolia* tree-ring width-based temperature reconstruction for the Mt. Dongda region, Northwest China, and its relationship to large-scale climate forcing, PLoS One, 11, e0160963, https://doi.org/10.1371/journal.pone.0160963, 2016.

Liu, Y., Lei, Y., Sun, B., Song, H. M., and Li, Q.: Annual precipitation variability inferred from tree-ring width chronologies in the Changling–Shoulu region, China, during AD 1853–2007, Dendrochronologia, 31, 290–296, https://doi.org/10.1016/j.dendro.2013.02.001, 2013.

Liu, Y., Won-Kyu, P., Cai, Q. F., Jung-Wook, S., and Hyun-Sook, J.: Monsoonal precipitation variation in the East Asia since A.D. 1840—tree-ring evidences from China and Korea, Science in China Series D: Earth Sciences, 46, 1031–1039, https://doi.org/10.1007/BF02959398, 2003.

Liu, Y., Ma, L. M., Cai, Q. F., An, Z. S., Liu, W. G., and Gao, L. Y.: Reconstruction of summer temperature (June-August) at Mt. Helan, China, from tree-ring stable carbon isotope values since AD 1890, Science in China Series D: Earth Sciences, 45, 1127–1136, https://doi.org/10.1360/02yd9109, 2002.

Liu, Y., Cai, Q. F., Liu, W. G., Yang, Y. K., Sun, J. Y., Song, H. M., and Li, X. X.: Monsoon

precipitation variation recorded by tree-ring $\delta^{18}O$ in arid Northwest China since AD 1878, Chemical Geology, 252, 56–61, https://doi.org/10.1016/j.chemgeo.2008.01.024, 2008.

Liu, Y., Cai, Q. F., Shi, J. F., Hughes, M. K., Kutzbach, J. E., Liu, Z. Y., Ni, F. B., and An, Z. S.: Seasonal precipitation in the south-central Helan Mountain region, China, reconstructed from tree-ring width for the past 224 years, Canadian Journal of Forest Research, 35, 2403–2412, https://doi.org/10.1139/x05-168, 2005.

Liu, Y., Shi, J. F., Shishov, V., Vaganov, E., Yang, Y. K., Cai, Q. F., Sun, J. Y., Wang, L., and Djanseitov, I.: Reconstruction of May–July precipitation in the north Helan Mountain, Inner Mongolia since A.D. 1726 from tree-ring late-wood widths, Chin. Sci. Bull., 49, 405–409, https://doi.org/10.1007/BF02900325, 2004.

Ma, L. M., Liu, Y., Cai, Q. F., and An, Z. S.: The precipitation records from tree-ring late wood width in the helan mountain, Marine geology & Quaternary geology, 23, 109–114 (In Chinese with English abstract), https://doi.org/10.16562/j.cnki.0256-1492.2003.04.016, 2003.

Ma, M. J., Pu, Z. X., Wang, S. G., and Zhang, Q. A.: Characteristics and numerical simulations of extremely large atmospheric boundary-layer heights over an arid region in north-west china, Boundary-Layer Meteorology, 140, 163–176, https://doi.org/10.1007/s10546-011-9608-2, 2011.

Ma, Z. G. and Fu, C. B.: The basic facts of aridity in northern China from 1951 to 2004, Chin. Sci. Bull., 51, 2429–2439 (In Chinese), https://doi.org/10.1360/csb2006-51-20-2429, 2006.

Ou, T. H. and Qian, W. H.: Vegetation variations along the monsoon boundary zone in East Asia, Chinese Journal of Geophysics, 49, 698–705 (In Chinese with English abstract), 2006.

Qin, L., Liu, G. X., Li, X. Z., Chongyi, E., Li, J., Wu, C. R., Guan, X., and Wang, Y.: A 1000-year hydroclimate record from the Asian summer monsoon-Westerlies transition zone in the northeastern Qinghai-Tibetan Plateau, Clim. Change, 176, 1–20, https://doi.org/10.1007/s10584-023-03497-1, 2023.

Qu, W. J., Zhang, X. H., Wang, D., Shen, Z. X., Mei, F. M., Cheng, Y., and Yan, L. W.: The important significance of westerly wind study, Marine Geology and Quaternary Geology, 24, 125–132 (In Chinese with English abstract), https://doi.org/10.16562/j.cnki.0256-1492.2004.01.018, 2004.

Shao, X. M., Xu, Y., Yin, Z. Y., Liang, E. Y., Zhu, H. F., and Wang, S.: Climatic implications of a 3585-year tree-ring width chronology from the northeastern Qinghai-Tibetan Plateau, Quaternary Science Reviews, 29, 2111–2122, https://doi.org/10.1016/j.quascirev.2010.05.005, 2010.

Sun, D. H., An, Z. S., Su, R. H., Deer, H. Y., and Sun, Y. B.: The dust deposition records of the evaluation of Asia monsoon and Westerly circulation in north China in the last 2.6Ma, Science in China (Series D), 33, 497–504 (In Chinese), 2003.

Sun, L. Q., Li, T. J., Li, Q. L., and Wu, Y. P.: Responses of autumn flood peak in the Yellow River source regions to westerly circulation index, Journal of Glaciology and Geocryology, 41, 1475–1482 (In Chinese with English abstract), https://doi.org/10.7522/j.issn.1000-0240.2019.0028, 2019.

Tang, X., Qian, W. H., and Liang, P.: Climatic features of boundary belt for East Asian Summer Monsoon, Plateau Meteorology, 25, 375–381 (In Chinese with English abstract), 2006.

Vicente-Serrano, S.M., Beguería, S. and López-Moreno, J.I.: A multiscalar drought index sensitive to global warming: the standardized precipitation evapotranspiration index. J. Clim., 23(7): 1696–1718, https://doi.org/10.1175/2009jcli2909.1., 2010.

Wang, B. J., Huang, Y. X., He, J. H., and Wang, L. J.: Relation between vapour transportation in the period of East Asian Summer Monsoon and drought in Northwest China. Plateau Meteorology, 23, 912–917 (In Chinese with English abstract), 2004.

Wang, J. L., Yang, B., Ljungqvist, F. C., Luterbacher, J., Osborn, Timothy j., Briffa, K. R., and Zorita, E.: Internal and external forcing of multidecadal Atlantic climate variability over the past 1,200 years, Nature Geoscience, 10, 512–517, https://doi.org/10.1038/ngeo2962, 2017.

Wang, K. L., Jiang, H., and Zhao, H. Y.: Atmospheric water vapor transport from westerly and monsoon over the Northwest China, Advances in Water Science, 16, 432–438 (In Chinese with English abstract), https://doi.org/10.14042/j.cnki.32.1309.2005.03.021, 2005.

Wigley, T.M.L., Briffa, K.R., Jones, P.D. On the average value of correlated time series, with applications in dendroclimatology and hydrometeorology. Journal of Climate and Applied Meteorology 23(2), 201–213, 1984.

Xiao, S. C., Chen, X. H., and Ding, A. J.: Study process of climate changes, environment evolution and its driving mechanism in the last two centuries in the Alxa Desert, Journal of Desert Research, 37, 1102–1201 (In Chinese with English abstract), 10.7522/j.issn.1000-694x.2017.00002, 2017.

Xiao, S. C., Yan, C. Z., Tian, Y. Z., Si, J. H., Ding, A. J., Chen, X. H., Han, C., and Teng, Z. Y.: Regionalization for desertification control and countermeasures in the Alxa Plateau, China, Journal of Desert Research, 39, 182–192 (In Chinese with English abstract), https://doi.org/10.7522/j.issn.1000-694X.2019.00068, 2019.

Xu, J. J., Wang, K. L., Jiang, H., Li, Z. G., Sun, J., Luo, X. P., and Zhu, Q. L.: A numerical simulation of the effects of Westerly and Monsoon on precipitation in the Heihe River Basin, Journal of Glaciology and Geocryology, 32, 489–496 (In Chinese with English abstract), 2010.

Yan, H. S., Hu, J., Fan, K., and Zhang, Y. J.: The analysis of relationship between the variations of Westerly Index in summer and precipitation during the flood period over China in the last 50 years. , Chinese Journal of Atmospheric Science, 31, 717–726 (In Chinese with English abstract), 2007.

Yang, B., Qin, C., Wang, J. L., He, M. H., Melvin, T. M., Osborn, T. J., and Briffa, K. R.: A

3,500-year tree-ring record of annual precipitation on the northeastern Tibetan Plateau, Proc. Natl. Acad. Sci. USA, 111, 2903–2908, https://doi.org/10.1073/pnas.1319238111, 2014.

Yang, J. H., Zhang, Q., Liu, X. Y., Yue, P., Shang, J. L., Ling, H., and Li, W. J.: Spatial-temporal characteristics and causes of summer precipitation anomalies in the transitional zone of typical summer monsoon, China, Chinese Journal of Geophysics, 62, 4120–4128 (In Chinese with English abstract), https://doi.org/10.6038/cjg2019M0639, 2019.

Yuan, L.: Hazards history in northwestern China, Gansu people's press, Lanzhou, China1994.

Zhang, F., Chen, Q. M., Su, J. J., Deng, Y., Gao, L. L., and Gou, X. H.: Tree-ring recorded of the drought variability in the northwest monsoon marginal, China, Journal of Glaciology and Geocryology, 39, 245–251 (In Chinese with English abstract), https://doi.org/10.7522/j.issn.1000-0240.2017.0028, 2017.

Zhang, Q., Yang, J. H., Wang, P. L., Yu, H. P., Yue, P., Liu, X. Y., Lin, J. J., Duan, X. Y., Zhu, B., and Yan, X. Y.: Progress and prospect on climate warming and humidification in Northwest China, Chin. Sci. Bull., 68, 1814–1828, https://doi.org/10.1360/TB-2022-0643, 2023.

Zhang, Q. B., Cheng, G. D., Yao, T. D., Kang, X. C., and Huang, J. G.: A 2,326 year tree-ring record of climate variability on the northeastern Qinghai-Tibetan Plateau, Geophys. Res. Lett., 30, 1739, https://doi.org/10.1029/2003GL017425, 2003.

Zhang, Q. L., Liu, W. G., Liu, Y., Ning, Y. F., and Wen, Q. B.: Relationship between the stable carbon and oxygen isotopic compositions of tree ring in the Mt. Helan region, Northwestern China, Geochimica, 34, 51–56, https://doi.org/10.19700/j.0379-1726.2005.01.006, 2005a.

Zhang, S., Xu, H., Lan, J. H., Goldsmith, Y., Torfstein, A., Zhang, G. L., Zhang, J., Song, Y. P., Zhou, K. E., Tan, L. C., Xu, S., Xu, X. M., and Enzel, Y.: Dust storms in northern China during the last 500 years, Science China Earth Sciences, 64, 813–824, https://doi.org/10.1007/s11430-020-9730-2, 2021.

Zhang, Y., Shao, X. M., Yin, Z. Y., Liang, E. Y., Tian, Q. H., and Xu, Y.: Characteristics of extreme droughts inferred from tree-ring data in the Qilian Mountains, 1700-2005, Clim. Res., 50, 141–159, https://doi.org/10.3354/cr01051, 2011.

Zhang, Y. X., Yu, L., and Yin, H.: Annual precipitation reconstruction over last 191 years at the south edge of Badain Jaran Desert based on tree ring width data, Desert and Oasis Meteorology, 9, 12–16 (In Chinese with English abstract), https://doi.org/10.3969/j.issn.1002-0799.2015.01.003, 2015.

Zhang, Y. X., Gou, X. H., Hu, W. D., Peng, J. F., and Liu, P. X.: The drought events recorded in tree ring width in Helan Mt. over past 100 years, Acta Ecologica Sinica, 25, 2121–2126 (In Chinese with English abstract), 2005b.